

Origin of InGaN light-emitting diode efficiency improvements using chirped AlGaIn multi-quantum barriers

Joachim Piprek^{1,a)} and Z. M. Simon Li²

¹NUSOD Institute LLC, P.O. Box 7204, Newark, Delaware 19714, USA

²Crosslight Software Inc., 121-3989 Henning Drive, Burnaby, British Columbia V5C 6P8, Canada

(Received 4 December 2012; accepted 3 January 2013; published online 17 January 2013)

We analyze efficiency droop reductions in InGaN/GaN light-emitting diodes caused by a chirped AlGaIn/GaN multi-quantum barrier (MQB). Such electron barriers are expected to create an additional forbidden energy range above the natural conduction band edge, which reduces the electron leakage current. Advanced numerical device simulations reveal that energy band bending practically eliminates this MQB effect. Instead, we find that the measured efficiency improvement has its origin in enhanced hole injection, which can be more easily accomplished using a single thin AlGaIn layer. © 2013 American Institute of Physics. [<http://dx.doi.org/10.1063/1.4776739>]

GaN-based light-emitting diodes (LEDs) are currently of immense interest for applications in lighting, displays, sensing, biotechnology, medical instrumentation, and other areas. However, the development of high-brightness GaN-based LEDs is handicapped by a significant efficiency reduction with increasing injection current. This efficiency droop phenomenon currently receives great attention but the physical mechanisms behind it are still under debate.¹ The two most frequently cited explanations for the droop are Auger recombination within the multi-quantum well (MQW) active region² and electron leakage from the MQW into the p-doped layers of the LED,³ resulting in poor hole injection into the MQW. A large number of proposals can be found in the recent literature on how to reduce the efficiency droop, in particular, by design optimization of the AlGaIn electron blocking layer (EBL), which is used to limit electron leakage into the p-doped side of the LED. Some of these publications utilize a multi-quantum barrier (MQB) comprising thin alternating layers of GaN and AlGaIn. Compared to one thick AlGaIn EBL of the same composition, MQBs were demonstrated to improve the performance of nitride-based LEDs and laser diodes.^{4–8}

The MQB concept is based on the quantum-mechanical reflection of electron waves by superlattice structures, similar to the light reflection by distributed Bragg reflectors. MQBs create a forbidden energy range above the natural conduction band edge, thereby increasing the effective electron barrier height. The MQB concept was first developed for GaInAsP-based laser diodes and LEDs.⁹ Later, a chirped MQB structure with slightly changing layer thickness was shown to eliminate the resonant electron tunneling that burdens a periodic MQB¹⁰ and to provide better AlGaInP LED performance.¹¹ But the measured performance improvements often deviated from the theoretical expectations,^{12,13} mainly due to MQB deformations typically found in real devices.

Using advanced numerical simulation, we here analyze recently published measurements on GaN-based LEDs with two alternative MQB structures, a periodic MQB and a chirped MQB.⁸ Compared to the bulk EBL, the periodic

MQB improved the LED efficiency, but the chirped MQB provided the highest efficiency and the lowest droop. The authors attributed the improved performance to enhanced electron reflection, but our analysis shows that electron reflection has a negligible influence. We find that the measured efficiency enhancement is mainly caused by improved hole injection. Based on these findings, we propose an EBL concept featuring a single 1-nm-thin undoped AlGaIn (i-AlGaIn) layer.

Our analysis utilizes a modified version of the APSYS simulation software.¹⁴ This software is widely used to study GaN-based LEDs.^{3,6,15} It self-consistently solves the semiconductor carrier transport equations, coupled to the photon emission from the strained quantum wells. The transport model considers drift and diffusion of electrons and holes, Fermi statistics, thermionic emission at hetero-interfaces, as well as a recently extended quantum tunneling model, which includes electron reflection above the MQB conduction band edge and hole reflection below the MQB valence band edge. Schrödinger and Poisson equations are solved iteratively in order to account for the quantum well deformation with changing device bias, both in the MQW active region and in the MQB region. Our model also considers the contribution of MQW Auger recombination to the LED efficiency droop. The coefficients of Auger and Shockley-Reed-Hall (SRH) recombination are adjusted to find agreement with measurements (see below). The built-in polarization charge density is calculated using a recently published second-order model,¹⁶ resulting in the built-in MQB interface charge density of $6.8 \times 10^{12} \text{ cm}^{-2}$ in our case. Further details of our model can be found elsewhere.^{17,18}

First, we simulate the conventional and the chirped MQB LED according to the design specifications given.⁸ A 3 μm -thick n-doped GaN layer ($5 \times 10^{18} \text{ cm}^{-3}$ Si) is followed by an undoped MQW active region comprising eight 2-nm-thick $\text{In}_{0.12}\text{Ga}_{0.88}\text{N}$ wells and nine 15-nm-thick GaN barriers. In the reference device, a conventional p-doped 45-nm-thick $\text{Al}_{0.15}\text{Ga}_{0.85}\text{N}$ EBL is grown on top of the MQW, covered by a p-GaN cap layer ($12 \times 10^{18} \text{ cm}^{-3}$ Mg). In the chirped MQB device, the 45-nm-thick AlGaIn layer is replaced by a MQB structure in which the AlGaIn layer thickness increases (0.75 nm, 3.375 nm, 6 nm, 8.625 nm, and

^{a)}piprek@nusod.org.

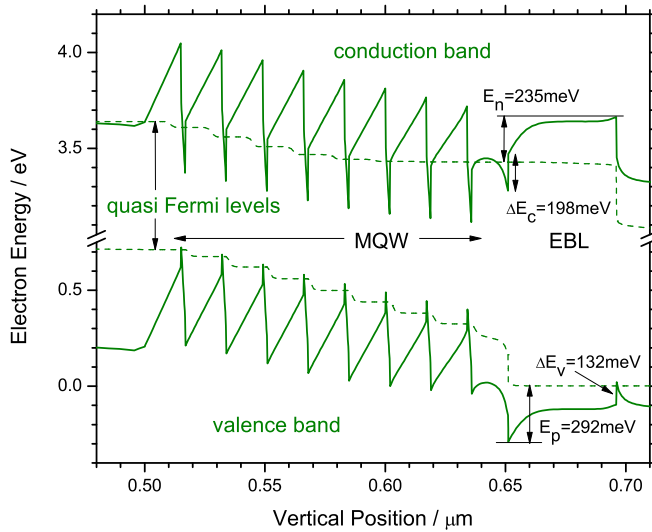


FIG. 1. Vertical electron energy band diagram near the active region of the EBL reference device (current density = 400 A/cm^2). The dashed lines mark the quasi Fermi levels, ΔE_c and ΔE_v are the EBL conduction and valence band offset, respectively, and E_n and E_p are the EBL energy barrier for electrons and holes, respectively.

11.25 nm) and the GaN layer thickness decreases (6.5625 nm, 4.6875 nm, 2.8125 nm, and 0.9375 nm) in growth direction.⁸ In both cases, the total thickness of the electron blocking structure is 45 nm.

Figure 1 plots the energy band diagram of the reference device. Interface polarization charges, ionized donors and acceptors, free carriers, as well as the applied bias lead to strong deviations from the ideal rectangular shape of the band edge profiles. Despite the EBL band offset ratio $\Delta E_c:\Delta E_v = 60:40$, the EBL energy barrier E_p for hole injection is significantly larger than the barrier E_n for electron leakage. Internal quantum efficiency (IQE) vs. current characteristics are plotted in Fig. 2. The reference device with bulk EBL exhibits an efficiency droop of 48% at the maximum current of 160 mA, which is in very good agreement with the measured droop of 48.5%.⁸ It is commonly assumed that the efficiency droop is not influenced by the photon

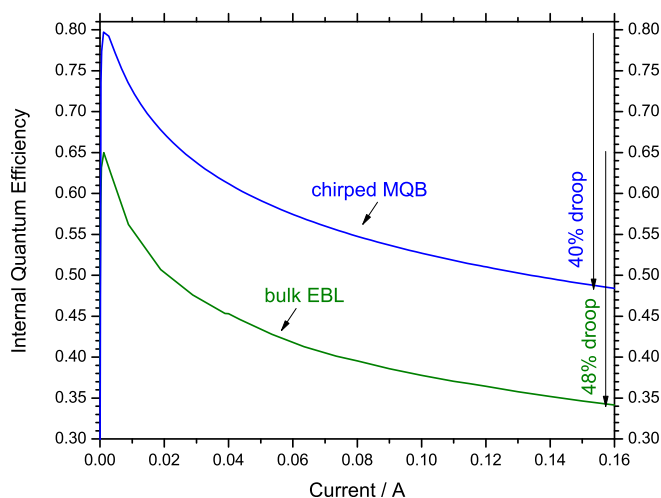


FIG. 2. Calculated internal quantum efficiency vs. current. The efficiency droop is measured relative to the peak efficiency. The maximum current density is 400 A/cm^2 .

extraction efficiency,¹ so that the relative droop of the measured external quantum efficiency (EQE)⁸ is the same as that of the internal quantum efficiency. The chirped MQB exhibits a reduced droop of 40% in Fig. 2, which is close to the measured EQE droop of 42%,⁸ i.e., the MQB is slightly more effective in the simulation, as expected. For the EBL device, the simulations result in 33% electron leakage at the total current of 160 mA, while the chirped MQB eliminates electron leakage almost completely. The remaining efficiency droop is caused by MQW Auger recombination. With a SRH lifetime of 100 ns, the Auger coefficient C was used as a fit parameter, resulting in $C = 10^{-30} \text{ cm}^6/\text{s}$. Both numbers are within the range reported in the literature.¹

We now analyze the cause for the performance improvement with chirped MQB. An ideal rectangular MQB conduction band edge allows for simple solutions to the Schrödinger equation.¹¹ The resulting MQB reflectivity spectra are shown in Fig. 3 both for electron leakage and for hole injection. The 99% reflection barrier for electrons/holes is only 9 meV/2meV higher than the AlGaIn conduction/valence band edge.

However, the band edge profiles of the real device strongly deviate from the ideal picture. Figure 4 plots the conduction band edge $E_c(x)$ for the MQB region, including the top QW, combined with the corresponding MQB electron reflectivity spectrum. Due to the band bending, the conduction band barrier is now $E_n = 405 \text{ meV}$, much higher than the barrier in the reference device (Fig. 1) and also much higher than the built-in conduction band offset of $\Delta E_c = 198 \text{ meV}$. The reflection spectrum exhibits strong tunneling through the thin MQB barrier peaks. Figure 5 plots the valence band edge $E_v(x)$ for the MQB region, combined with the corresponding MQB hole reflectivity spectrum. The MQB energy barrier for hole injection is now $E_p = 307 \text{ meV}$, which is only slightly higher than the barrier in the reference device (Fig. 1) but substantially lower than the electron barrier E_n in Fig. 4. The hole reflectivity spectrum also exhibits tunneling dips near the thin MQB barrier peaks.

As the net effect of carrier tunneling and reflection is hard to estimate from Figs. 4 and 5, we simply removed it from the model and compared the resulting performance to

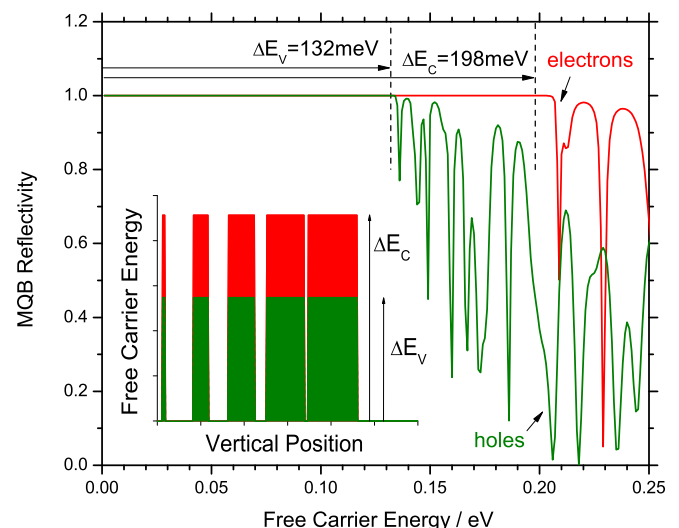


FIG. 3. Electron and hole reflectivity spectra for the ideal chirped MQB. The inset shows the profile of the MQB conduction and valence band edges.

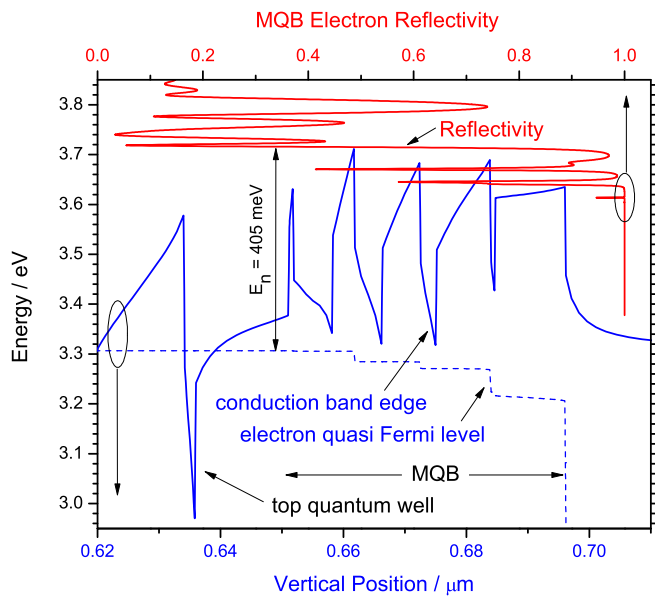


FIG. 4. Conduction band edge profile near the chirped MQB and MQB electron reflectivity spectrum simulated at 400 A/cm^2 .

the IQE curve in Fig. 2. Both IQE curves are identical. Thus, quantum mechanical MQB effects do not contribute to the elimination of the electron leakage by the chirped MQB. Instead, the increased electron barrier energy E_n seems mainly responsible, caused by the lower electron quasi Fermi level, i.e., by a strongly reduced electron density of $0.05 \times 10^{18} \text{ cm}^{-3}$ on the left-hand side (LHS) of the MQB (Fig. 4).

For further analysis, we now replace the MQB with a 1-nm-thin undoped AlGaIn layer. Surprisingly, the IQE characteristic is identical to the MQB curve in Fig. 2. The band diagram in Fig. 6 shows an i-AlGaIn electron barrier of $E_n = 394 \text{ meV}$ that is almost the same as with chirped MQB (Fig. 4). The LHS electron density at the thin EBL is only $0.06 \times 10^{18} \text{ cm}^{-3}$, compared to $26 \times 10^{18} \text{ cm}^{-3}$ in the reference device. As a consequence, the actual electron leakage is

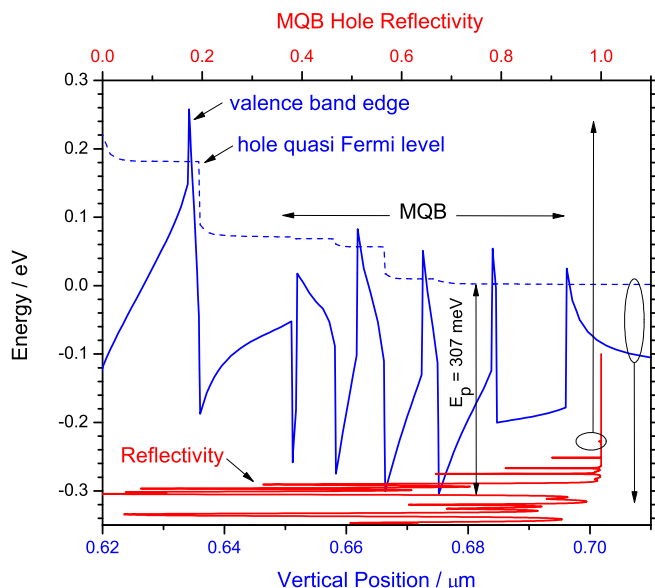


FIG. 5. Valence band edge profile near the chirped MQB and MQB hole reflectivity spectrum simulated at 400 A/cm^2 .

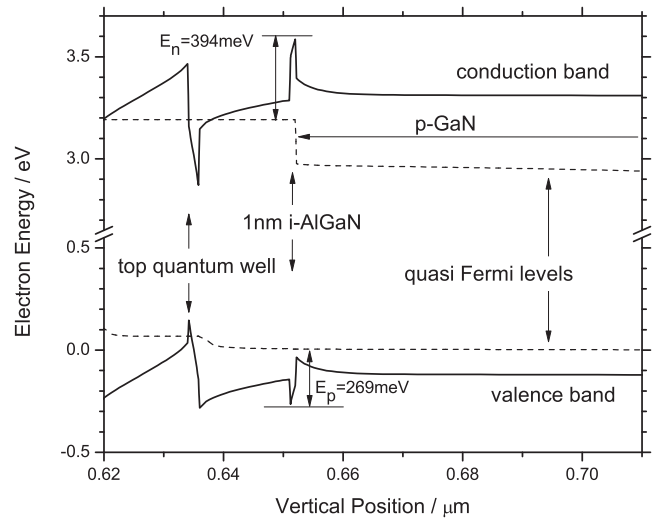


FIG. 6. Energy band diagram near the 1-nm-thin EBL at 400 A/cm^2 .

only 0.2% of the total current of 160 mA, despite the high probability of electron tunneling through the thin EBL. In contrast, the density of free holes on the right-hand-side (RHS) of the thin EBL is close to 10^{19} cm^{-3} , as indicated by the upward bending of the valence band edge toward the hole Fermi level (Fig. 6). This high density of free holes is mainly attracted by the negative interface polarization charges at the RHS of the i-AlGaIn layer. In addition, the hole barrier $E_p = 269 \text{ meV}$ is now lower than in the reference device. Due to their larger effective mass, the tunnel probability of holes is generally smaller than that of electrons. But the strong hole accumulation at the thin EBL still causes a significant tunnel injection into the MQW. We confirmed this unexpected dominance of hole tunneling over electron tunneling with simple analytical tunnel models for rectangular barriers¹⁹ using the band offsets and the quasi Fermi levels from Fig. 6. Disabling the hole tunneling in the APSYS simulation results in strong electron leakage. Thus, RHS hole accumulation and hole tunneling through the thin AlGaIn layer are found to be the key mechanism for the observed efficiency enhancement. As more holes reach the MQW, less electrons leak out, resulting in electron depletion at the EBL and an enhanced barrier energy E_n . In other words, electron leakage is not a cause but rather a consequence of poor hole injection.

The single thin layer allows for even better hole injection than the MQB since hole tunneling is not restricted to MQB quantum levels. But with this device example, the chirped MQB already eliminates the electron leakage, so the thin i-AlGaIn layer cannot improve the IQE characteristic in Fig. 2 any further. For the same reason, a higher i-AlGaIn band gap or a lower thickness do not give better IQE results in this case. But growing the i-AlGaIn thickness to 3 nm results in larger electron leakage of about 2% at 160 mA since the hole tunneling probability is reduced. Dropping the Al content of the 1-nm layer from 0.15 to 0.10 gives a similarly enhanced electron leakage, because the lowered interface polarization charge density attracts less holes.

Complete removal of the EBL in our simulation leads to a dramatic rise in electron leakage, i.e., a strongly reduced hole injection, since the p-GaN hole density is now much

smaller. This finding is in agreement with previous measurements of ultra-violet LED efficiency improvements after insertion of an 1-nm-thin i-AlN layer below the p-side cladding layer.²⁰

In summary, we show by advanced numerical device simulation that the LED efficiency improvement achieved with chirped MQB electron blocking layers is caused by enhanced hole injection into the MQW and not by electron reflection, as commonly assumed. We propose to use a very thin single i-AlGaIn layer instead of the MQB to further improve hole injection.

¹J. Piprek, *Phys. Status Solidi A* **207**, 2217 (2010).

²Y. C. Shen, G. O. Mueller, S. Watanabe, N. F. Gardner, A. Munkholm, and M. R. Krames, *Appl. Phys. Lett.* **91**, 141101 (2007).

³M. H. Kim, M. F. Schubert, Q. Dai, J. K. Kim, E. F. Schubert, J. Piprek, and Y. Park, *Appl. Phys. Lett.* **91**, 183507 (2007).

⁴S. N. Lee, S. Y. Cho, H. Y. Ryu, J. K. Son, H. S. Paek, T. Sakong, T. Jang, K. K. Choi, K. H. Ha, M. H. Yang, O. H. Nam, and Y. Park, *Appl. Phys. Lett.* **88**, 111101 (2006).

⁵H. Hirayama, Y. Tsukada, T. Maeda, and N. Kamata, *Appl. Phys. Express* **3**, 031002 (2010).

⁶Y. Y. Zhang and Y. A. Yin, *Appl. Phys. Lett.* **99**, 221103 (2011).

⁷Y. Y. Zhang, X. L. Zhu, Y. A. Yin, and J. Ma, *Electron. Devices Lett.* **33**, 994 (2012).

⁸Y. Y. Lin, R. W. Chuang, S. J. Chang, S. Li, Z. Y. Jiao, T. K. Ko, S. J. Hon, and C. H. Liu, *Photon. Technol. Lett.* **24**, 1600 (2012).

⁹K. Iga, H. Uenohara, F. Koyama, *Electron. Lett.* **22**, 1008 (1986).

¹⁰H. Fujii, K. Endo, and H. Hotta, *Appl. Phys. Lett.* **64**, 3479 (1994).

¹¹C. S. Chang, Y. K. Su, S. J. Chang, P. T. Chang, Y. R. Wu, K. H. Huang, and T. P. Chen, *J. Quantum Electron.* **34**, 77 (1998).

¹²P. Raisch, R. Winterhoff, W. Wagner, M. Kessler, H. Schweizer, T. Riedl, R. Wirth, A. Hangleiter, and F. Scholz, *Appl. Phys. Lett.* **74**, 2158 (1999).

¹³M. R. Brown, R. J. Cobley, K. S. Teng, P. Rees, S. P. Wilks, A. Sobiesierski, P. M. Smowton, and P. Blood, *J. Appl. Phys.* **100**, 084509 (2006).

¹⁴See www.crosslight.com for APSYS by Crosslight Software Inc.

¹⁵Y.-K. Kuo, T.-H. Wang, and J.-Y. Chang, *Appl. Phys. Lett.* **100**, 031112 (2012).

¹⁶J. Pal, G. Tse, V. Haxha, M. A. Migliorato, and S. Tomic, *Phys. Rev. B* **84**, 085211 (2011).

¹⁷J. Piprek and S. Li, "GaIn-based light-emitting diodes," in *Optoelectronic Devices: Advanced Simulation and Analysis*, edited by J. Piprek (Springer, New York, NY, 2005), Ch. 10.

¹⁸J. Piprek, *Proc. SPIE* **8262**, 82620E (2012).

¹⁹J. Piprek, *Semiconductor Optoelectronic Devices—Introduction to Physics and Simulation* (Academic, San Diego, CA, 2003), p. 55.

²⁰J. Zhang, Y. Sakai, and T. Egawa, *J. Quantum Electron.* **46**, 1854 (2010).